

Crystal and electronic structures and electrical, magnetic, and optical properties of two copper tetrahalide salts of bis(ethylenedithio)-tetrathiafulvalene

I. R. Marsden, M. L. Allan, and R. H. Friend

Cavendish Laboratory, University of Cambridge, Madingley Road, Cambridge CB3 0HE, United Kingdom

M. Kurmoo, D. Kanazawa, and P. Day

The Royal Institution of Great Britain, 21 Albemarle Street, London W1X 4BS, United Kingdom

G. Bravic and D. Chasseau

Laboratoire de Cristallographie et Physique Cristalline, Université Bordeaux I, 351, Cours de la Libération, F-33405 Talence, France

L. Ducasse

Laboratoire de Physico-Chimie Théorique, Université Bordeaux I, 351, Cours de la Libération, F-33405 Talence, France

W. Hayes

Clarendon Laboratory, University of Oxford, Parks Road, Oxford OX1 3PU, United Kingdom

(Received 25 October 1993; revised manuscript received 4 April 1994)

We report the crystal and electronic band structures at 295 K and measurements of temperature-dependent magnetic susceptibility, electron paramagnetic resonance, optical reflectivity, conductivity, and thermopower for two copper tetrahalide salts of bis(ethylenedithio)-tetrathiafulvalene (BEDT-TTF), (BEDT-TTF)₃CuBr₄ and (BEDT-TTF)₃CuCl₂Br₂. The two salts are isostructural with layers of BEDT-TTF having charges of 0 and $+e$ separated by layers of pseudo-square-planar tetrahalides of copper (II). At ambient pressure these salts show conductivities near 1 S cm^{-1} , and the magnetic properties indicate coupled localized spins present on both BEDT-TTF and the d^9 copper layers. At 60 K, there is a discontinuous drop in susceptibility, a sharpening of the electron paramagnetic resonance linewidth, and an increase in g value that we attribute to the loss of the contribution from the BEDT-TTF sheets. This may be associated with a Jahn-Teller distortion of the planar copper complexes. Below the transition temperature the susceptibility can be fitted to a quadratic layer antiferromagnet with $J=15 \text{ K}$ (CuBr₄) and 8 K (CuCl₂Br₂) and one spin per formula unit. Under pressure there is a very rapid increase in conductivity, to 500 S/cm at 24 kbar, the largest increase of conductivity under pressure in any molecular solid yet studied. There is a sharp transition from metal to insulator at temperatures rising to 111 K near 5 kbar, and falling to 80 K at 20 kbar. We consider that these salts are nearly metallic at ambient pressure, with strongly enhanced susceptibilities, but are brought to a fully metallic state under pressure as a result of increased intermolecular contacts.

I. INTRODUCTION

Organic charge transfer salts now provide a very wide range of model electronic materials, with properties ranging from metallic and superconducting behavior through to nonmetallic magnetically ordered materials. The charge transfer salts formed with bis(ethylenedithio)-tetrathiafulvalene (BEDT-TTF) have provided an important series of materials, particularly regarding superconducting properties,^{1,2} and examples have been prepared with a very wide range of anions. The most common structural motifs in such salts are sheets of BEDT-TTF donors, sometimes arranged as one-dimensional chains, separated by sheets of the anions. Intermolecular contacts within the BEDT-TTF sheets are responsible for the formation of delocalized carriers and the metallic behavior when found. The primary effect of the anion is to control the packing of the BEDT-TTF donors, and

systematic studies of structural changes brought about by selection of modified anions have produced the two families of superconducting salts; the β polytype 2:1 salts formed with linear anions^{3,4} and the κ polytype 2:1 salts formed with polymeric anions.⁵ However, other properties can be introduced by selection of the anion, and we and other groups⁶⁻¹⁴ have made salts with anions containing magnetic moments localized on transition-metal ions. The interaction of local magnetic moments on the anions with the delocalized conduction electrons in the organic sheets is of considerable interest, and it is for this reason that we have investigated the copper tetrahalide salts that form the subject of this paper. We note that there are at present relatively few coupled magnetic and/or superconductor materials; examples included erbium rhodium boride, ErRh₄B₄ and some of the Chevrel phases, e.g., HoMo₆S₈.¹⁵⁻¹⁷

Although our goal was to make superconducting salts

containing these paramagnetic anions, none has been isolated so far; in general they are semiconductors. In most cases the electron transport is confined to the BEDT-TTF layers while the magnetic properties are defined by the sum of two magnetic sublattices, the conduction electrons on the BEDT-TTF moiety and the unpaired spins on the anions. For example, in $(\text{BEDT-TTF})_3\text{CuCl}_4 \cdot \text{H}_2\text{O}$, the only salt with a magnetic anion to show metallic behavior,⁸ we have demonstrated that there is a very weak interaction between the two kinds of spin, while for the semiconducting salt $(\text{BEDT-TTF})_2\text{FeCl}_4$ and insulating salt $(\text{BEDT-TTF})\text{FeBr}_4$,⁷ there is no measurable interaction. By contrast, in the present case, we present evidence for a strong interaction between the two sublattices in the BEDT-TTF series, as well as structural phase transitions of the anions from planar (D_{2d}) to distorted tetrahedral (C_{2v}) that modify the electronic structure and thus the electrical and magnetic properties.¹⁸

The CuBr_4^{2-} and $\text{CuCl}_2\text{Br}_2^{2-}$ salts investigated here were selected because the CuCl_4^{2-} salt mentioned above had shown interesting metallic behavior. However, this new salt is very different structurally from the CuCl_4^{2-} salt, and their electronic properties are unrelated. Whereas the CuCl_4^{2-} anions are distorted from square planar, as is usually expected for Jahn-Teller d^9 ion (the *trans* Cl-Cu-Cl angle being 150°), the anions in the new salts are, very unusually, undistorted pseudosquare planar at room temperature (though we have evidence that the Jahn-Teller distortion is present at low temperatures). It is to our knowledge the first complex of CuBr_4^{2-} found to be planar.^{19,20} It is interesting that the stoichiometry of all the salts is 3:1, which in terms of charge is 3:2 for comparison with the β and κ phases; and that for the CuCl_4^{2-} salt a water molecule is included to make up the size of the cavities formed between the BEDT-TTF layers.

The room temperature crystal structure of a CuBr_4^{2-} salt of BEDT-TTF has previously been determined by Mori *et al.*²¹ The crystal belongs to the monoclinic space group $P2_1/c$ with the long needle axis parallel to the crystallographic b axis; two independent BEDT-TTF molecules were observed with different bond lengths, which Mori *et al.* assigned charges of 0 and $\frac{3}{4}e^+$, respectively. The model used for the structural refinement was based on a composition $(\text{BEDT-TTF}^0)_2(\text{BEDT-TTF}^{3/4+})_4\text{Cu}^{\text{I}}\text{Br}_2\text{Cu}^{\text{II}}\text{Br}_4$ with equivalent Cu-Br distances for both oxidation states of the copper atom. The stacking of the donor molecules resembles that of the α polytype of the tri-iodide salt.²² However, some ambiguity remained in the estimation of both the charge separation and the bromine atom population in the crystal structure refinement and this was noted as the cause for the high R value. In addition, the above stoichiometry cannot account for the number of unpaired electrons per formula unit observed in the susceptibility measurements.^{18,13} In the present paper we resolve this problem by redetermining the crystal structure of the bromide salt and fully characterizing the structure of the newly synthesised isostructural mixed halide salt.

Taking advantage of new structural informations, we report the calculated electronic band structure and a full range of magnetic, transport, and optical measurements on single crystals of $(\text{BEDT-TTF})_3\text{CuBr}_4$ and $(\text{BEDT-TTF})_3\text{CuCl}_2\text{Br}_2$ both at ambient pressure and in the case of transport studies as a function of hydrostatic pressure up to 24 kbar. Some of the results have been reported in a preliminary publication.¹⁸

II. EXPERIMENT

BEDT-TTF was prepared by the method of Larsen and Lenoir²³ and recrystallized twice from chloroform before use. The tetra-alkyl ammonium salts of the anions were obtained by reacting CuBr_2 and $(\text{R}_4\text{N})\text{X}$ ($\text{X} = \text{Cl}$ or Br) in absolute ethanol. The purity was checked by elemental analysis before use. The charge transfer salt was obtained by electrocrystallization of BEDT-TTF (20 mg) in a benzonitrile solution (50 ml) of $[(\text{C}_2\text{H}_5)_4\text{N}]_2\text{CuBr}_4$ or $[(\text{CH}_3)_4\text{N}]_2\text{CuBr}_2\text{Cl}_2$ (200 mg). A three-compartment cell with platinum wire electrodes was used, with a constant applied current of 1-2 μA for two weeks. The crystals were black shiny needles of dimension $4 \times 1 \times 0.2 \text{ mm}^3$.

Several synthetic routes for the preparation of the CuBr_4^{2-} salt exist. Mori *et al.* obtained the CuBr_4 salt by electrocrystallisation of BEDT-TTF and $\text{Cu}^{\text{I}}\text{Br}_2^-$ in 112-trichloroethane, and Susuki *et al.* by diffusion of BEDT-TTF and $\text{Cu}^{\text{II}}\text{Br}_2$ in benzonitrile or acetonitrile. While in the former the BEDT-TTF as well as the anion need to be oxidized to give the product, for the latter the CuBr_2 is used as the oxidant and the source of the anion.

We have used the most direct method; applying a potential low enough to oxidize only the organic molecules. When the anions and BEDT-TTF are mixed together in chlorinated solvents such as 112-trichloroethane, dichloromethane, or chloroform, we noted that all the BEDT-TTF is consumed within a short time to give black microcrystals without even passing a current. The salt $(\text{BEDT-TTF})_3\text{Cu}^{\text{II}}\text{Br}_4 \cdot \text{Br}_3$ has been identified as one of the products from 12-dichloroethane;²⁴ it crystallizes in the orthorhombic group ($Pccn$). In benzonitrile, however, the reaction is slow, such that crystals of the titled compounds are formed on the electrode. In this paper all the measurements were conducted on single crystals harvested from the electrodes of several cells.

The band structure was calculated from transfer integrals obtained by the extended Hückel method. The highest occupied molecular orbitals (HOMO's) are generated from the dimer splitting method.²⁵

Electrical conductivity was measured using four-probe techniques, with high-pressure measurements performed in a clamp pressure cell with pentane-isopentane (1:1) mixture as the pressure transmitting medium.²⁶ Conductivity measurements were limited to the long axis (b) of the needle crystals. Contacts were made with silver paint on evaporated gold pads. Data were collected using both ac and dc techniques. Thermopower was measured using similar contacts with a temperature gradient of typically 1 K across the crystals, and corrected for the absolute thermopower of the gold contact wires.

Electron paramagnetic resonance spectra were mea-

sured on several single crystals as a function of angle and temperature. Crystals were mounted on a cut flat face of Spectrosil Quartz rod using a smear of silicone grease. The spectrometer is a Varian E9 operating at a microwave frequency of 9 GHz and 100 kHz field modulation. Variable temperature (4–300 K) were obtained by use of a continuous flow Oxford Instrument cryostat and an ITC-4 temperature controller. The field was calibrated with a diphenylpicrylhydrozyl standard.

Static magnetic susceptibility measurements were made on two independent batches of randomly oriented crystals of ~ 2 mg each. Data were recorded for cooling and warming runs as well as for different applied magnetic fields on a Faraday balance employing a Cahn microbalance. Data were corrected for the core diamagnetism and a small amount of ferromagnetic impurities.

Optical reflectivity was measured on a Perkin Elmer 1710 spectrometer equipped with an IR plan microscope operating in the range $400\text{--}4300\text{ cm}^{-1}$ and a Perkin Elmer Lambda 9 ($3000\text{--}50\,000\text{ cm}^{-1}$). The data were normalized to that of a gold mirror. A KRS5 and a calcite polarizer were employed for the mid- to near-infrared and visible regions, respectively.

III. RESULTS

A. Crystal structure

The compounds are isostructural belonging to the monoclinic system (Fig. 1), $P2_1/c$, $a = 17.001(3)$, $b = 10.140(2)$, $c = 14.178(3)$ Å, $\beta = 102.75(2)^\circ$, $V = 2383(1)$ Å³, $d_c = 2.14\text{ g/cm}^3$ for $(\text{BEDT-TTF})_3\text{CuBr}_4$, and $a = 16.895(3)$, $b = 10.108(4)$, $c = 14.150(4)$ Å, $\beta = 102.60(2)^\circ$, $V = 2358(1)$ Å³, $d_c = 2.04\text{ g/cm}^3$ for $(\text{BEDT-TTF})_3\text{CuBr}_2\text{Cl}_2$. The volume of the unit cell found by Mori *et al.*²¹ lies in between those of the CuBr_4

and CuBr_2Cl_2 salts suggesting that there might be some chlorine in their compound. If so, the chlorine must come from the solvent (*vide infra*), a synthetic problem that has been encountered previously.^{27,28}

The final refinement using the atomic coordinates of Mori *et al.*²¹ as the starting point for the two compounds results in lower values of the reliability R factor (0.034 and 0.036) and subsequently to smaller standard deviations on atomic coordinates. Here we have also refined the occupancy factor of the halogen atoms. The high precision of the present results allows us to assert that the occupancy factor of the bromine atoms is 100% for the $(\text{BEDT-TTF})_3\text{CuBr}_4$ salt and that in the case of the CuCl_2Br_2 salt it is possible to differentiate the positions of the chlorine and the bromine atoms, with occupancy factors of 50%. This confirms, contrary to what was assumed by Mori *et al.* that the two copper atoms in the unit cell are in oxidation state two. As the copper atom lies on an inversion center, the CuBr_4^{2-} and $\text{CuBr}_2\text{Cl}_2^{2-}$ anions are strictly planar. The Cu-Br distances are 2.407 and 2.421 Å in $(\text{BEDT-TTF})_3\text{CuBr}_4$ and equal to 2.394 and 2.389 Å in CuBr_2Cl_2 while Cu-Cl distances are found to be 2.309 and 2.313 Å. Note that the average $\text{Cu}^{\text{II}}\text{-Cl}$ is 2.24 Å and $\text{Cu}^{\text{II}}\text{-Br}$ is 2.38 Å,²⁹ while $\text{Cu}^{\text{I}}\text{-Cl}$ and $\text{Cu}^{\text{I}}\text{-Br}$ are 2.107 and 2.226 Å, respectively.³⁰ Due to the two independent bond lengths, both anions have a D_{2d} symmetry.

Two crystallographically independent BEDT-TTF molecules (A and B) were observed in both compounds; the difference in the bond lengths and comparison with BEDT-TTF salts with well-defined charges strongly suggest that the charges of A and B are, respectively, 0 and $+e$. The two salts consist of layers of BEDT-TTF, stacked in a $ABBAB$ manner, separated by pseudosquare planar tetrahalides of copper (II) (Fig. 1). Complete details of the crystal structure are given elsewhere.^{31,32}

B. Electronic band structure

The transfer integrals and the calculated band structure of $(\text{BEDT-TTF})_3\text{CuBr}_4$ are given in Fig. 2. They were found to be very different from those published by Mori *et al.*²¹ The energy dispersion is quite small along the c direction in relation to the transfer integrals shown. This small dispersion together with the average charge of $2/3e +$ per BEDT-TTF molecule implies that the four lowest bands are completely filled. The calculated electronic structure corresponds to a semiconductor with a small gap of ~ 5 meV. This result might be expected from the previous discussion about the existence of two crystallographically independent molecules with different oxidation states.

Several other BEDT-TTF salts exhibit the same zigzag stacking as those under study, for example, the two forms of $(\text{BEDT-TTF})_2\text{Ag}(\text{CN})_2$,³³ $\theta\text{-(BEDT-TTF)}_2\text{I}_3$,³⁴ $\alpha\text{-(BEDT-TTF)}_2\text{I}_3$,²² and $\alpha\text{-(BEDT-TTF)}_2\text{MHg}(\text{SCN})_4$.³⁵ In particular, the θ phase and the $\text{Ag}(\text{CN})_2$ salts have quite similar transfer integrals and Fermi surfaces. It appears that the Hg salt and the CuBr_4 salt bear some similarities together with striking differences. Within the stack, the

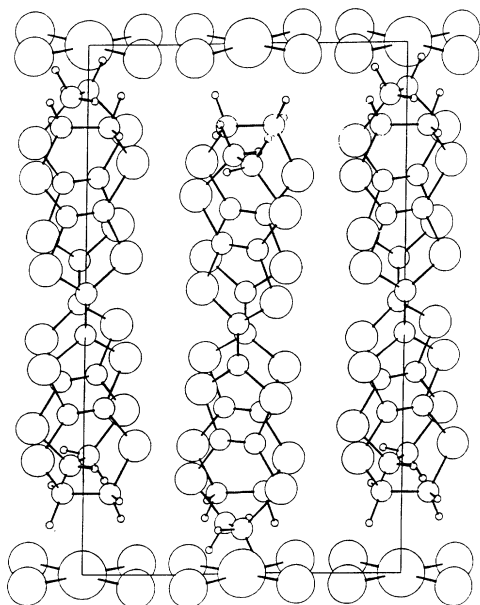


FIG. 1. View of the crystal structure of $(\text{BEDT-TTF})_3\text{CuBr}_4$ along the c axis.

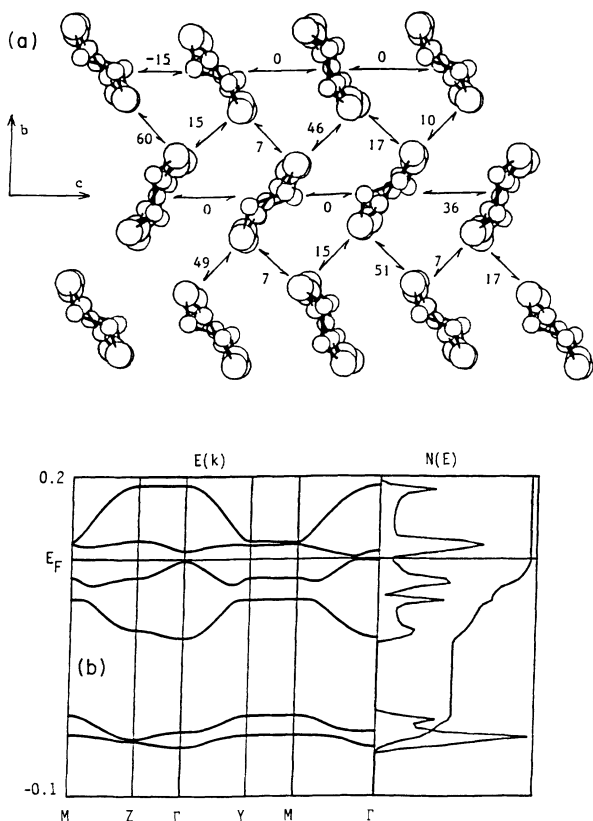


FIG. 2. (a) View of the structure along the central C=C bonds showing the calculated transfer integrals (meV). (b) Band structure and density of state calculated from the transfer integrals. Dispersion is shown within the plane of the BEDT-TTF sheets.

transfer integrals may be large with positive or negative values or even close to zero, depending on small differences in the shifts along the long molecular axis or along the short one; in $(\text{BEDT-TTF})_3\text{CuBr}_4$ they are close to zero while they are much larger in the Hg salt. The interstack interactions are also much stronger in the Hg salt than in the CuBr_4 salt. These results, together with the different molecular charges in CuBr_4 , lead to a band structure for a semiconductor while that for the Hg salt corresponds to a metal.

C. Transport properties

The room-temperature conductivities along the *b* axis of the two materials are very similar, being 0.7(1) S/cm, a low value for metallic organic conductors of the BEDT-TTF family, and a high value for the semiconductors. At ambient pressure the conductivity of both salts decreases steadily on cooling with no evidence of any sharp transitions, as shown in Fig. 3. However closer examination of the data shows a gradual change in the activation energy on lowering the temperature and two more slight changes in the activation energy at ca. 60 and 50 K.

Application of pressure to both compounds has a dramatic effect on the absolute value of the conductivity

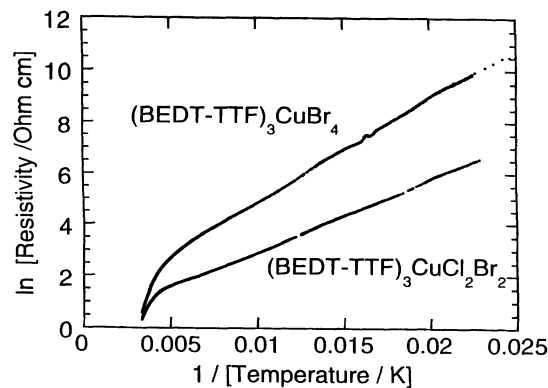


FIG. 3. Log_e (resistivity) measured along the *b* axis vs reciprocal temperature at ambient pressure.

as well as on the phase transitions, as shown in Ref. 18. In fact, these two materials show the largest change in conductivity on application of pressure of all known organic conducting solids. The conductivities of both increase almost linearly at a rate of 25 (S/cm)/kbar up to about 8 kbar finally attaining a plateau of approximately 500 times the ambient pressure value at 22 kbar. As we discuss later, we consider that at ambient pressure these salts are just on the insulating side of the Mott-Hubbard transition, and that pressure rapidly brings them into the metallic regime. This change in character is seen also in the temperature dependence of the conductivity, which increases with decreasing temperature above 7 kbar. The two salts show similar behavior. The temperature dependence of the conductivities along the needle axis (*b*) of the crystals of the CuBr_4^{2-} salt is shown at several pressures in Fig. 4, that for the $\text{CuCl}_2\text{Br}_2^{2-}$ salt is presented in Ref. 18. At low temperatures there is clear evidence for the presence of phase transitions that take both salts from the

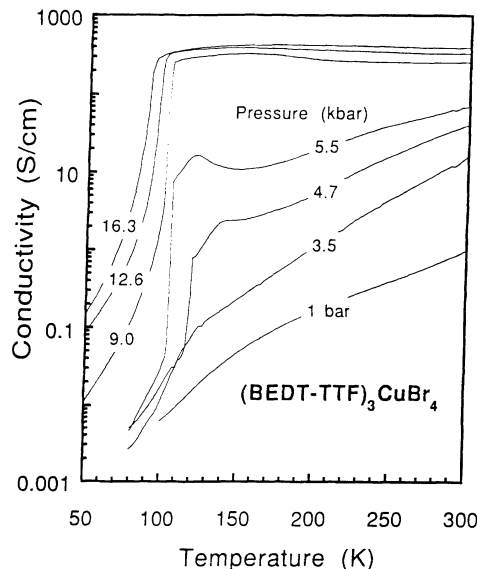


FIG. 4. Temperature dependence of the *b*-axis conductivity of $(\text{BEDT-TTF})_3\text{CuBr}_4$ at several pressures.

metallic to a readily observable semiconducting regime. The sharp transition to the low-temperature semiconductor phase is readily observable at pressures above about 3 kbar, where it occurs at around 80 K in both materials. The transition temperature rises to a little above 100 K near 6 kbar, and falls gradually to around 80 K by 20 kbar. We note that there is some structure in the temperature dependence of the conductivity just above the transitions, seen particularly clearly around 5 kbar, it is possible that they are associated with changes in pressure at the freezing point of the pressure medium, which is about 0.7 kbar for this pressure system.

The temperature dependence of the thermopower measured with the temperature gradient along the b axis has been shown in Ref. 18. Although the thermopower is very low near room temperature, it becomes large and negative on cooling, reaching values of -120 and -230 $\mu\text{V}/\text{K}$ near 170 K. These large values indicate that the materials are semiconductors, and the size of the thermopower being similar to that measured in some of the α' BEDT-TTF salts that behave as Mott-Hubbard insulators.³⁶ We note that the thermopower is larger in the bromide salt, as is the activation energy of the conductivity, see Fig. 3.

D. Optical properties

The polarized reflectivity spectra parallel and perpendicular to the needle axis (b) are shown in Fig. 5. The spectra are characterized by sharp vibrational structures on a strong electronic background centered around 2000 cm^{-1} . Many more intermolecular BEDT-TTF vibrational modes are observed than in those salts with one crystallographically independent molecule per unit cell, indicating that we are observing modes belonging to the two independent molecules of different electronic charge in the unit cell. For example, the C-S stretching mode,³⁷ $\nu_{49}(b_{2u})$ in the β , κ , and α' polytype, in which the BEDT-TTF molecules carry a charge of $\frac{1}{2}e^+$, is at 884 cm^{-1} ,³⁸ which for a charge of $\frac{2}{3}+$ is at 892 cm^{-1} (BEDT-TTF)₃[ReO₄]₂, and for $+e$, in (BEDT-TTF)Ag₄(CN)₅ and (BEDT-TTF)FeBr₄ it is observed at 900 cm^{-1} . Neutral BEDT-TTF has a band at 770 cm^{-1} .

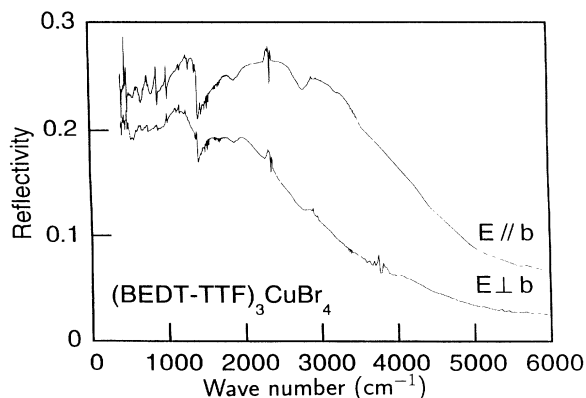


FIG. 5. Optical reflectivity in the midinfrared region for (BEDT-TTF)₃CuBr₄ at room temperature for $E \parallel b$ and $E \perp b$.

Thus the peaks at 768 and 896 cm^{-1} can be assigned to vibrational modes of (BEDT-TTF)⁰ and (BEDT-TTF)⁺, respectively, while the broad band at ~ 2000 cm^{-1} arises from an intraband transition. Unfortunately the C=C region is more difficult to interpret; the shapes and frequencies of the bands vary with the electronic nature of the compound in question.

In the visible region the spectra are dominated by charge transfer (ligand to metal) and $d-d$ transitions. The spectrum for $E \parallel b$ (Fig. 6), has been studied down to 30 K. There is a gradual sharpening of the spectrum on lowering the temperature such that at 30 K, there are four features (6200 , 8000 , 17500 , and 20000 cm^{-1}). Kramers-Krönig transformation of the data reveals a redshift of 200 – 300 cm^{-1} in the peak at 17500 cm^{-1} from 300 to 30 K. A Jahn-Teller distortion of the CuBr_4^{2-} would result in a lowering of the energy of the $d-d$ transition as has been observed for the CuCl_4^{2-} .³⁹ These values are of the right order of magnitude for the observed increase in the g values.

E. Magnetic properties

1. Static susceptibility

The temperature dependence of the bulk magnetic susceptibilities of the two compounds, shown in Fig. 7, are very similar. At high temperatures the susceptibilities obey a Curie-Weiss law with $\theta \sim -110$ K (CuBr_4^{2-}) and -59 K ($\text{CuCl}_2\text{Br}_2^{2-}$). The susceptibility of the bromide salt decreases abruptly between 58 – 60 K, and shows a rounded maximum at ~ 30 K indicative of short-range antiferromagnetic order. The susceptibility of the mixed halide salt shows a similar abrupt decrease between 53 and 56 K and a maximum at ~ 10 K. At the abrupt transition, the susceptibilities of both salts fall by a similar amount (2.5×10^{-3}) emu/mol formula unit. A change in the g values, of the magnitude reported below would give an increase in susceptibility of 2.7% , whereas the observed decrease is an order of magnitude larger.

Below 50 K the temperature dependence of the susceptibility of the bromide salt can be fitted by a model of a quadratic layer antiferromagnet (QLAF) with 0.95 spins per formula unit and $J = 15$ K.⁴⁰ This shows that below the transition there are two unpaired electrons per unit cell (note that $z = 2$) that interact two dimensionally, with a temperature-independent J . The susceptibility of the mixed-halide salt likewise fits the QLAF model between 15 and 55 K with 1.0 spins per formula unit and $J = 8$ K. The anisotropy of the g value at 30 K (Ref. 41) indicates that below the 60 -K transition the spins are mainly localized on Cu^{II} . The antiferromagnetic interaction between the spins of the copper atoms is probably mediated by the electrons on the BEDT-TTF layers through a superexchange mechanism, which may be responsible for the observation of a single line in the electron paramagnetic resonance (EPR) spectra. The shortest Cu-Cu distance is ~ 8.7 Å and the halogen atoms on neighboring anions are at least ~ 4.3 Å apart. The J values of the two salts in this temperature range depend on the extent to which the copper atoms interact with the BEDT-TTF mole-

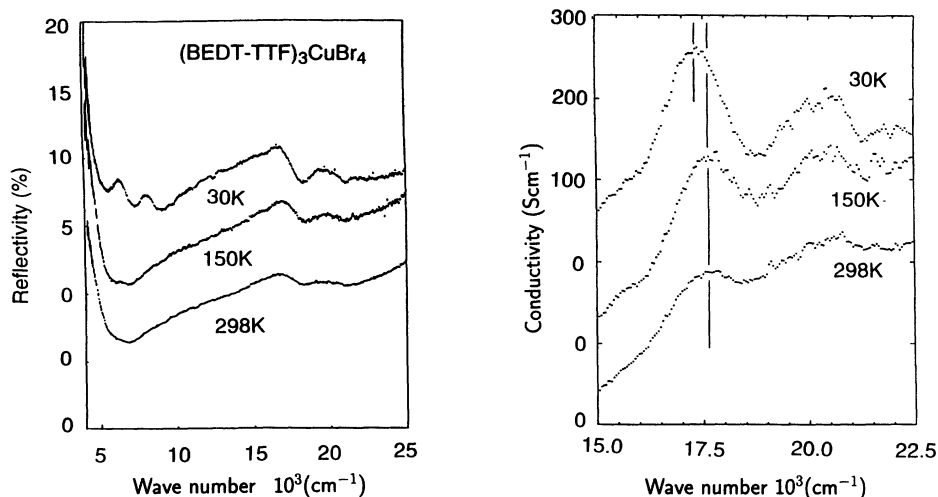


FIG. 6. Visible region optical reflectivity and conductivity for $(\text{BEDT-TTF})_3\text{CuBr}_4$ with $E \parallel b$.

cules. Clearly the interaction is stronger in the bromide ($\theta = -110$ and $J = 15$ K) than in the mixed halide salt ($\theta = -59$ and $J = 8$ K), in agreement with the fact that bromine is larger and more polarizable than chlorine. The similarity between the two salts is even more marked when an extrapolation of the low-temperature behavior is subtracted from the high-temperature data:¹⁸ the residual susceptibility of the two salts is almost identical.

2. EPR

The spin susceptibility, g -value, and peak-to-peak linewidth of the resonance line have been derived from the spectra as a function of temperature and angle to the applied field. At all temperatures and crystals' orientations the spectra of both materials are dominated by a single resonance line.^{41,42} The temperature-dependent data were recorded along three orthogonal axes, the crystallographic axis b and c and a^* . The angular dependences of the spectra of the two materials are similar while those of the spin susceptibility differ marginally at

low temperatures. In both cases, there is an abrupt change in linewidth, g value, and integrated area at ca. 60 K. The changes in the spectra for the bromide salt take place over a temperature range of ca. 10 K (Fig. 8). A loss of intensity of the wide peak and an increase for the narrow peak is observed on lowering the temperature through the transition. For the mixed halide the transition takes place over a wider temperature range.

The angular dependences of the g values at room temperature show uniaxial symmetry with the principal values $g_{\parallel} = 2.070$ and $g_{\perp} = 2.021$ for the CuBr_4^{2-} salt and $g_{\parallel} = 2.085$ and $g_{\perp} = 2.016$ for the $\text{CuCl}_2\text{Br}_2^{2-}$ salt. These values lie close to the mean of those of the square planar Cu ion and BEDT-TTF cation, for example, square planar CuBr_4^{2-} doped in PdBr_4^{2-} has g values⁴³ $g_{\parallel} = 2.143$ and $g_{\perp} = 2.044$ while for $(\text{BEDT-TTF})_2\text{I}_3$ the g values are $g_1 = 2.0011$, $g_2 = 2.0065$, and $g_3 = 2.0025$.⁴⁴ At ~ 30 K, below the phase transition, the g values $g_{\parallel} = 2.110$ and $g_{\perp} = 2.040$ for the CuBr_4^{2-} salt are close to those for the nonplanar ion in

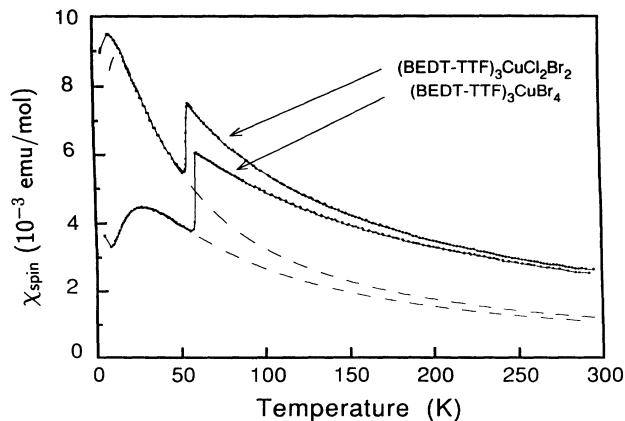


FIG. 7. Static magnetic susceptibility for randomly oriented samples of the copper tetrahalide salts. Broken lines are fits to the quadratic layer antiferromagnet model discussed in the text. Susceptibilities are shown in emu/mol formula unit.

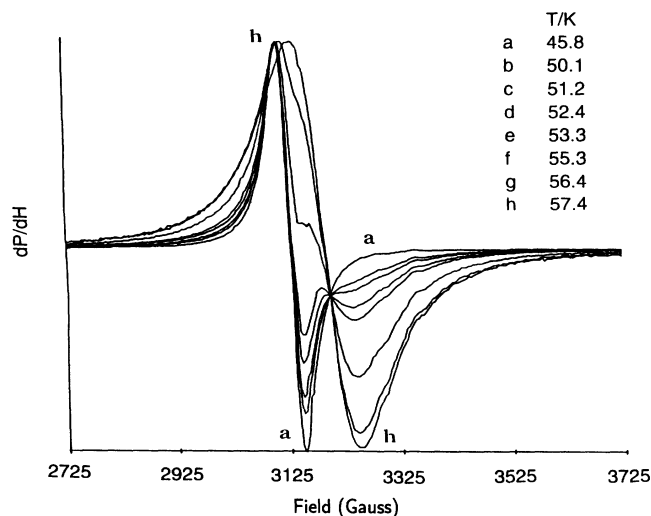


FIG. 8. EPR spectra of $(\text{BEDT-TTF})_3\text{CuBr}_4$ at various temperatures through the phase transition near 60 K, with the static field parallel to the b axis.

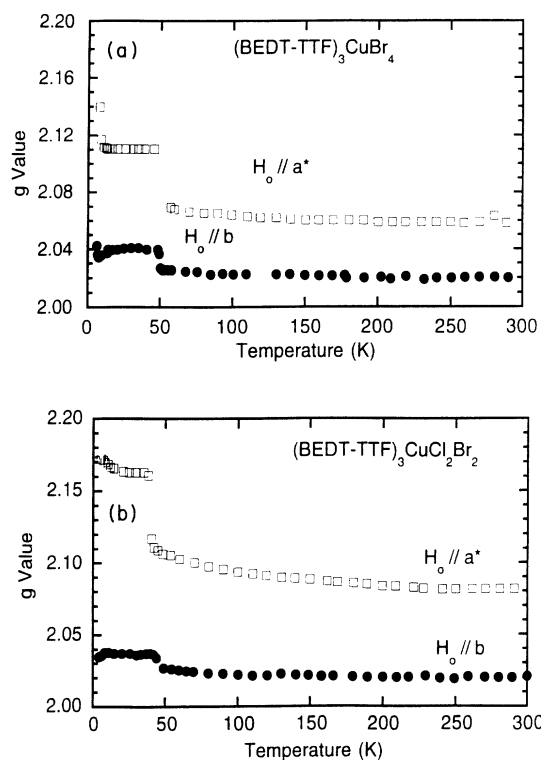


FIG. 9. Temperature dependence of the two g values of the copper tetrahalide salts.

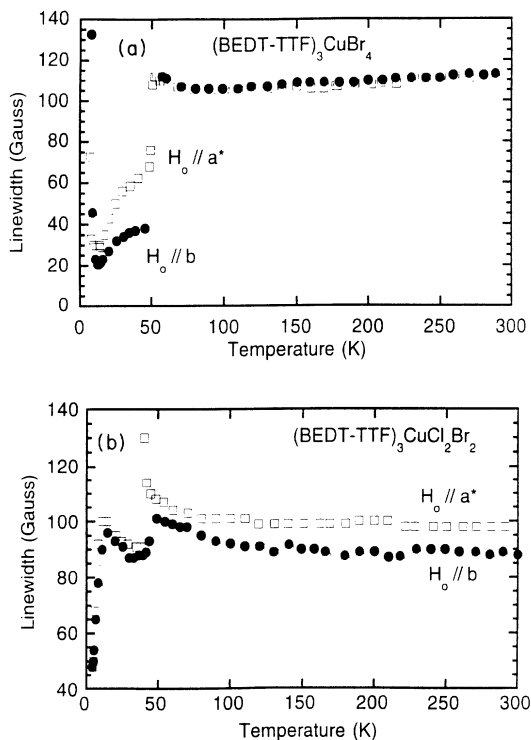


FIG. 10. Temperature dependence of the EPR linewidths measured parallel and perpendicular to the b axis.

$[\text{NH}_3(\text{CH}_2)_n\text{NH}_3][\text{CuBr}_4]$, $g_{\parallel}=2.097$ and $g_{\perp}=2.047$.⁴⁵

The angular dependences of the g values at room temperature show uniaxial symmetry with the principal values $g_{\parallel}=2.070$ and $g_{\perp}=2.021$ for the CuBr_4^{2-} salt and $g_{\parallel}=2.085$ and $g_{\perp}=2.016$ for the $\text{CuCl}_2\text{Br}_2^{2-}$ salt. These values lie close to the mean of those of the square planar CuBr_4^{2-} doped in PdBr_4^{2-} has g values⁴³ $g_{\parallel}=2.143$ and $g_{\perp}=2.044$ while for $(\text{BEDT-TTF})_2\text{I}_3$ the g values are $g_1=2.0011$, $g_2=2.0065$, and $g_3=2.0025$.⁴⁴ At ~ 30 K, below the phase transition, the g values $g_{\parallel}=2.110$ and $g_{\perp}=2.040$ for the CuBr_4^{2-} salt are close to those for the nonplanar ion in $[\text{NH}_3(\text{CH}_2)_n\text{NH}_3][\text{CuBr}_4]$, $g_{\parallel}=2.097$ and $g_{\perp}=2.047$.⁴⁵

The temperature dependence of the g values of both salts is shown in Fig. 9: that of the bromide salt divides into three regions; one between 60 and 300 K, the second between 8 and 60 K, and the third below 8 K, while in the $\text{CuCl}_2\text{Br}_2^{2-}$ salt we find only the first two regions with a transition temperature of ~ 40 K. The angular dependence of the g values above and below the transition at ~ 50 K is similar except for the slightly larger values below the transition. The divergence of the g value and the linewidth (*vide supra*) of the CuBr_4^{2-} salt is indicative of a three-dimensional magnetic ordering.

The linewidths of the two materials (Fig. 10) behave differently; that of the CuBr_4^{2-} salt does not show any dispersion while the $\text{CuCl}_2\text{Br}_2^{2-}$ shows a weak dispersion with orientation at room temperature. Below the transition, the reverse is observed. In both cases, the linewidth is constant from 300 K to the transition temperature, though there is sign of softening of the lattice near the transition. Below the transition at ~ 50 K the two salts behave quite differently. For the CuBr_4^{2-} salt, the linewidth decreases on lowering temperature to a minimum at ~ 8 K, where there is a sudden divergence within a few degrees. The latter is associated with an increase of the g value. For the $\text{CuCl}_2\text{Br}_2^{2-}$ salt, the linewidth increases to maximum at ~ 15 K and a gradual lowering to low temperature.

IV. DISCUSSION

Our calculated transfer integrals and band structure on the CuBr_4 salt are very different from those of Mori *et al.*²¹ We find several zero transfer integrals [Fig. 2(a)] due to the large slip of the molecules with respect to one another along the short molecular axis, similar to that found for $(\text{BEDT-TTF})_3\text{CuCl}_4\cdot\text{H}_2\text{O}$.⁸ Note that the interstack transfer integral along the b axis is greater than those within the stacks. This is found to be the case in most of the BEDT-TTF salts, and results in higher conductivities perpendicular to the stacking axis. With the 3:2 stoichiometry, assuming divalent copper tetrahalide anions, the BEDT-TTF HOMO bands are two-thirds filled, and also with six BEDT-TTF molecules within the unit cell, which requires four of the six bands to be filled. In contrast, the calculation of Mori *et al.* leads to three degenerate bands with very small dispersion; the band filling assuming the correct stoichiometry would result in

a semiconductor on the border line being a metal. Our calculation leads to six well-dispersed bands. Whether this gives a semiconductor or semimetal depends on the band dispersions, and we find here that the Fermi energy lies between the fourth and fifth bands with a minimum semiconducting gap at the zone center of ~ 5 meV. We note that the bands are calculated to be narrow, with a full bandwidth of less than 0.3 eV, and expect to see effect due to Coulomb interactions, as indeed is observed.

The two salts whose properties we have described are particularly interesting members of the BEDT-TTF series of charge transfer salts because they lie on the border line between metallic and semiconducting behavior. The room-temperature conductivities of about 1 S/cm, are too low for metallic behavior [the κ -phase superconducting materials such as the $\text{Cu}(\text{NCS})_2^-$ salts has conductivities an order of magnitude larger], and yet are very high for a semiconductor. The magnetic properties are also unusual in that, as we discuss further below, the susceptibility associated with the "conduction electrons" on the BEDT-TTF stacks is apparently very high. We consider that the jump of 2.5×10^{-3} emu/mole formula unit in susceptibility at the low-temperature transition is due to the loss of the contribution from these electrons, and we note that this is an exceptionally large susceptibility for salt of such a type. To account for a contribution of this magnitude to the susceptibility one must assume that two spins per formula unit which are both fully localized, and which are weakly antiferromagnetically coupled. Comparison can be made with the α' polytype such as $(\text{BEDT-TTF})_2\text{Ag}(\text{CN})_2$, in which there is one localized spin per dimer of BEDT-TTF and which shows quasi-one-dimensional antiferromagnetic coupling; peak susceptibilities at temperatures (60 K) comparable to the exchange coupling energy are 1.7×10^{-3} emu/mol formula unit. Note that the conduction electron susceptibility in a related 3:2 salt that exhibits metallic (and superconducting behavior under pressure), $(\text{BEDT-TTF})_3\text{Cl}_2 \cdot 2\text{H}_2\text{O}$, is only 7×10^{-4} emu/mole formula unit.⁴⁶

These facts suggest strongly that these materials are just on the insulator side of the Mott-Hubbard transition. Semiconducting behavior is not due to a gap in the one-electron density of states, but arises because the holes on the BEDT-TTF stacks localize due to the strong Coulomb interaction. The 3:2 charge stoichiometry of these salts requires that two holes are accommodated per three BEDT-TTF sites. Comparison of the bond lengths within the BEDT-TTF molecule with those of well-defined charges shows clearly that two of the BEDT-TTF molecules are charged and that one is close to neutral.

The transport properties are therefore those of a "magnetic" semiconductor, with the activation energy for conductivity identified as $U_{\text{eff}}/2$, where U_{eff} is the on-site Coulomb energy (Hubbard energy) associated with the transfer of a charge to place two changes on a single site. This model has been applied to the case of α' polytypes by Parker *et al.*³⁶ The activation energies measured for the copper tetrahalide salts are relatively low in comparison with the α' polytype salts, indicating that the Coulomb localization is weak. The size of the thermo-

power is consistent with this model.³⁶

The magnetic properties of these two salts are unusual. We note that only a single EPR line is seen, though there is clear evidence that this has contributions from both the localized d^9 copper moments and the localized moments present on the BEDT-TTF sites. For example, the g values above the low-temperature transition are intermediate between those expected for the copper moment and as found for spins on BEDT-TTF sites. This indicates that there is a significant level of interaction between the two spin systems, in contrast to the other magnetic anion salts which we have studied.^{7,8} Below the phase transitions seen in both salts around 60 K the susceptibilities are well fitted by a quadratic layer antiferromagnetic ordering model, and values for the exchange interaction of 15 and 8 K are found for $(\text{BEDT-TTF})_3\text{CuBr}_4$ and $(\text{BEDT-TTF})_3\text{CuCl}_2\text{Br}_2$, respectively. These values provide some indication of the strength of the exchange interactions present in these materials.

The phase transitions at 58–60 and 53–56 K in $(\text{BEDT-TTF})_3\text{CuBr}_4$ and $(\text{BEDT-TTF})_3\text{CuCl}_2\text{Br}_2$, respectively, cause the loss of a significant fraction of the susceptibility, change the g values close to those expected for copper d^9 ions, and cause a large reduction in linewidth. Below the transition the susceptibilities and g values are fully consistent with the presence of one spin per copper. We consider therefore that the higher susceptibility above the transition must result from a large contribution from the BEDT-TTF sheets. We do not have information about the low-temperature structure at present. However, a Jahn-Teller distortion of the square-planar copper tetrahalide is expected for this d^9 ion, and we propose that it is this that drives the change in properties observed here. The shift in the $d-d$ optical transitions is consistent with this change in copper environment. The most likely explanation for the loss of susceptibility from the BEDT-TTF sites is that there is pairing of the two spins present on two out of the three BEDT-TTF sites along the stacks.

The behavior of these salts under pressure shows a remarkable change from semiconductor to metallic properties. The increase in conductivity by a factor of 500 in 20 kbar is the highest such increase that we are aware of in molecular conductors, and takes these salts well into the domain of fully metallic behavior. It is certainly not surprising to see some increase in conductivity on cooling when the room-temperature conductivity has reached 500 S/cm. Such a very large increase in conductivity is only likely to be found when pressure transforms the material from one domain of behavior (magnetic insulator) to another (metal). Of the few other examples of materials which show comparable increases in conductivity under pressure, $\text{Cs}_{0.83}\{(\text{Pd}[\text{C}_2\text{S}_2(\text{CN})_2])\} \cdot 0.5\text{H}_2\text{O}$ (Refs. 47 and 48) shows an increase by a factor of 250 at 20 kbar, and we note that this is also attributed to a transition from Mott-Hubbard insulator to metal.

The low-temperature transition to a semiconducting state under pressure is very abrupt and indicates the presence of a phase transition. We consider that the Jahn-Teller distortion proposed to account for the ambient pressure properties is unlikely to be suppressed rapidly

under pressure, hence it is very likely that this transition is present and responsible for the metal to insulator transition. The Jahn-Teller distortion lowers symmetry, and it is likely that this further reduces symmetry at the BEDT-TTF sites, possibly by setting up a superlattice. The band structure shown in Fig. 2(b) will be modified under pressure principally through the broadening of the bands, and we expect the Fermi energy to continue to lie close to the band that is calculated at ambient pressure.

V. CONCLUSIONS

The two salts (BEDT-TTF)₃CuBr₄ and (BEDT-TTF)₃CuCl₂Br₂ reveal a range of properties new to this class of low-dimensional conductors. Evidence for cou-

pling of the spin states of the copper and BEDT-TTF stacks is very clear, and we observe a crossover from magnetic insulator to metal under modest hydrostatic pressures. Further work, particularly on the low-temperature structure, is in progress.

ACKNOWLEDGMENTS

We thank the Science and Engineering Research Council, CNRS, NATO, and the British Council for partial support of this work. We thank Dr. F. L. Pratt for useful discussions and comments. Laboratoire de Cristallographie et Physique Cristalline and Laboratoire de Physico-Chimie Théorique are URAs numbers 144 and 503 of CNRS.

- ¹D. Jérôme, *Science* **252**, 1509 (1991).
- ²J. M. Williams, A. J. Schultz, U. Geiser, K. D. Carlson, A. M. Kini, H. H. Wang, W. K. Kwok, M. H. Whangbo, and J. E. Schirber, *Science* **252**, 1501 (1991).
- ³E. B. Yagubskii, I. F. Shchegolev, V. N. Laukhin, P. A. Kononovich, M. V. Kartsovnik, A. V. Zvarykhina, and L. I. Buranov, *Pis'ma Zh. Eksp. Teor. Fiz.* **39**, 12 (1984) [*JETP Lett.* **39**, 12 (1984)].
- ⁴S. S. P. Parkin, E. M. Engler, S. R. R., R. Lagier, V. Y. Lee, J. C. Scott, and R. L. Greene, *Phys. Rev. Lett.* **50**, 270 (1983).
- ⁵H. Urayama, H. Yamochi, G. Saito, K. Nozawa, T. Sugano, M. Kinoshita, S. Saito, K. Oshima, A. Kawamoto, and J. Tanaka, *Chem. Lett.* **1988**, 55.
- ⁶M. Kurmoo, T. Mallah, P. Day, I. Marsden, M. Allan, R. H. Friend, F. L. Pratt, W. Hayes, D. Chasseau, J. Gaultier, and G. Bravic, in *The Physics and Chemistry of Organic Superconductors*, edited by G. Saito and S. Kagoshima, Springer Proceedings in Physics Vol. 51 (Springer, Berlin, 1990), p. 290.
- ⁷T. Mallah, C. Hollis, S. Bott, K. Kurmoo, P. Day, M. Allan, and R. H. Friend, *J. Chem. Soc. Dalton Trans.* **1990**, 859.
- ⁸P. Day, M. Kurmoo, T. Mallah, I. R. Marsden, R. H. Friend, F. L. Pratt, W. Hayes, D. Chasseau, G. Bravic, and L. Ducasse, *J. Am. Chem. Soc.* **114**, 10722 (1992).
- ⁹M. Kurmoo, P. Day, M. Allan, and R. H. Friend, *Mol. Cryst. Liq. Cryst.* (to be published).
- ¹⁰A. V. Gudenko, V. B. Ginodman, V. E. Korotkov, A. V. Koshelap, N. D. Kushch, V. N. Laukhin, L. P. Rozenberg, A. G. Khomenko, R. P. Shibaeva, and E. B. Yagubskii, in *The Physics and Chemistry of Organic Superconductors* (Ref. 6), p. 365.
- ¹¹T. Mori, P. Wang, K. Imeada, T. Enoki, H. Inokuchi, F. Sakai, and G. Saito, *Synth. Met.* **27**, A451 (1989).
- ¹²T. Sugano, H. Takenouchi, D. Shiomi, and M. Kinoshita, *Synth. Met.* **55-57**, 2217 (1993).
- ¹³K. Susuki, J. Yamaura, N. Sugiyasu, T. Enoki, and G. Saito, *Synth. Met.* **55-57**, 2191 (1993).
- ¹⁴C. Bellitto, M. Bonamico, and G. Staulo, *Mol. Cryst. Liq. Cryst.* **232**, 155 (1993).
- ¹⁵Author, in *Superconductivity in Ternary Compounds*, edited by M. B. Maple and Ø. Fischer (Springer, Berlin, 1982), Vol. 34.
- ¹⁶Author, in *Superconductivity in Magnetic and Exotic Materials*, edited by T. Matsubara and A. Kotani (Springer, Berlin, 1984), Vol. 52.
- ¹⁷K. P. Sinha and S. L. Kakani, *Magnetic Superconductors* (Nova, New York, 1989).
- ¹⁸M. Kurmoo, D. Kanazawa, P. Day, I. R. Marsden, M. Allan, and R. H. Friend, *Synth. Met.* **55-57**, 2347 (1993).
- ¹⁹A. C. Massabni, O. R. Nascimento, K. Halvorson, and R. D. Willett, *Inorg. Chem.* **31**, 1779 (1992).
- ²⁰K. Waizumi, H. Masuda, H. Einaga, and N. Fukushima, *Chem. Lett.* **1993**, 1145.
- ²¹T. Mori, F. Sakai, G. Saito, and H. Inokuchi, *Chem. Lett.* **1987**, 927.
- ²²K. Bender, I. Hennig, D. Schweitzer, K. Dietz, H. Endres, and H. J. Keller, *Mol. Cryst. Liq. Cryst.* **108**, 359 (1984).
- ²³J. Larsen and C. Lenoir, *Synthesis* **2**, 134 (1988).
- ²⁴M. B. Inoue, Q. Fernando, and M. Inoue, *Synth. Met.* **41-43**, 2069 (1991).
- ²⁵L. Ducasse, A. Abderrabba, J. Hoarau, M. Pesquer, B. Gallois, and J. Gaultier, *J. Phys. C* **19**, 3085 (1986).
- ²⁶D. R. P. Guy and R. H. Friend, *J. Phys. E* **19**, 430 (1986).
- ²⁷M. J. Rosseinsky, M. Kurmoo, D. R. Talham, P. Day, D. Chasseau, and D. Watkin, *J. Chem. Soc.* **1988**, 88.
- ²⁸M. Kurmoo, M. J. Rosseinsky, P. Day, P. Auban, W. Kang, D. Jerome, and P. Batail, *Synth. Met.* **27**, A425 (1989).
- ²⁹K. E. Halvorson, C. Patterson, and R. D. Willett, *Acta Crystallogr. Sec. B* **46**, 508 (1990).
- ³⁰M. Apslund, S. Jagner, and M. Nilsson, *Acta Chem. Scand. A* **37**, 57 (1983).
- ³¹P. Guionneau, G. Bravic, J. Gaultier, D. Chasseau, M. Kurmoo, D. Kanazawa, and P. Day, *Acta Crystallogr. Sec. C* (to be published).
- ³²S. Hebrard, G. Bravic, J. Gaultier, D. Chasseau, M. Kurmoo, D. Kanazawa, and P. Day, *Acta Crystallogr. Sec. C* (to be published).
- ³³M. Kurmoo, P. Day, A. M. Stringer, J. A. K. Howard, L. Ducasse, F. L. Pratt, J. Singleton, and W. Hayes, *J. Mater. Chem.* (to be published).
- ³⁴H. Kobayashi, R. Kato, A. Kobayashi, Y. Nishio, K. Kajita, and W. Sasaki, *Chem. Lett.* **1986**, 833.
- ³⁵H. Mori, S. Tanaka, M. Oshima, T. Mori, Y. Murayama, and H. Inokuchi, *Bull. Chem. Soc. Jpn.* **63**, 2183 (1990).
- ³⁶I. D. Parker, R. H. Friend, M. Kurmoo, and P. Day, *J. Phys. Condens. Matter* **1**, 5681 (1989).
- ³⁷K. Kornelsen, J. Eldridge, H. H. Wang, and J. M. Williams, *Solid State Commun.* **74**, 501 (1990).
- ³⁸F. L. Pratt, W. Hayes, M. Kurmoo, and P. Day, *Synth. Met.* **27**, A 439 (1989).
- ³⁹M. R. Bond, T. J. Johnson, and R. D. Willett, *Can. J. Chem.* **66**, 963 (1988).
- ⁴⁰M. E. Lines, *J. Phys. Chem. Solids* **31**, 101 (1970).
- ⁴¹M. Kurmoo, D. Kanazawa, and P. Day, *Synth. Met.* **41-43**, 2123 (1991).

- ⁴²M. Kurmoo, D. Kanazawa, and P. Day, in *Mixed Valency Systems: Applications in Chemistry, Physics and Biology*, edited by K. Prassides (Kluwer, Dordrecht, 1990), p. 419.
- ⁴³C. Chow, K. Chang, and R. D. Willett, *J. Chem. Phys.* **59**, 2629 (1973).
- ⁴⁴T. Sugano, G. Saito, and M. Kinoshita, *Phys. Rev. B* **34**, 117 (1986).
- ⁴⁵T. M. Kite and J. E. Drunheller, *Magn. Res.* **54**, 253 (1983).
- ⁴⁶S. D. Obertelli, I. R. Marsden, R. H. Friend, M. Kurmoo, M. J. Rosseinsky, P. Day, F. L. Pratt, and W. Hayes, in *The Physics and Chemistry of Organic Superconductors* (Ref. 6), p. 181.
- ⁴⁷I. D. Parker, R. H. Friend, and A. E. Underhill, *Synth. Met.* **29**, F195 (1989).
- ⁴⁸I. D. Parker, R. H. Friend, P. Clemenson, and A. E. Underhill, *Nature* **324**, 547 (1986).